1 MHZ BANDWIDTH, REAL-TIME SCHLIEREN TECHNIQUES IN A LINEAR TRANSONIC CASCADE

by

J.-J. CAMUS
Whittle Laboratory, Cambridge, U.K.

and

P.J. BRYANSTON-CROSS
Churchill College, Cambridge, U.K.

1. INTRODUCTION

One of the characteristic features of transonic flows is their unsteadiness (1)(2). This is often associated with the early stages of shock formation and, insofar as these shocks are weak, concomitant fluctuations may not be of any significance energetically. However, when these fluctuations affect dissipative structures, in shock-boundary layer interactions for example, they can only increase the rate of entropy production in the fluid.

The most obvious instance of highly unsteady dissipative flow in turbomachines is in the wake region of the blades. Linear cascades additionally suffer from the presence of free shear layers which can generate regular large pressure fluctuations at frequencies of several hundred Hz (3).

Study of these fast changing flows is only possible with large bandwidth instrumentation. Usually this means the use of hot wires or, more reliable in high speed flows, hot films. Examples of the current state of these techniques appear in refs. (4) and (5).

High-speed photography has also been used to good effect and, though such work is often not reported, an example appears in (8). Framing rates in that study were around 10^4 pps so, the effective bandwidth was considerably less. This was adequate to demonstrate regular movement of the shock pattern in the cascade at frequencies of 400 to 600 Hz.

The bandwith available from heated thin films appears to be around 20 kHz (5).

The speed of response required for the investigation of trailing edge flows is much in excess of this. Consider, for example, the formation of a stable vortex street in the wake of a blade of 1 mm trailing edge thickness$^{(d)}$. Assuming a typical gas velocity $^{(U)}$of 340 ms^{-1} and a Strouhal number$^{(St)}$ of 0.2 we have, from

$$St = fd/U$$

where f is the vortex frequency, f ≅ 70 kHz. (Fig.1).

Frequencies well in excess of this simple estimate have indeed been measured by Heinemann and Bütefisch (6). They reported vortex frequencies up to 160 kHz. Their method, first proposed in this context by Lawaczeck and Heinemann (7), consists in recording the fluctuating light level at one point in the schlieren image of the flow with a photomultiplier behind a pinhole in the screen on which the image is formed. The time resolution is then limited only by that of the photomultiplier and the spatial resolution by the sensitivity of the schlieren system.

We describe, in this communication, extensions of the techniques briefly described above. Firstly, it is shown that, taking trailing edge flow as an example, high speed photographic framing rates have to increase by an order of magnitude to resolve even the simplest details of the flow. Secondly, a new method of dynamic schlieren image analysis is described which exploits the advantages of two-point correlation across the image using two photomultipliers and a fast digital correlator.

2. EXPERIMENTAL DETAILS

(a) Cascade tunnel

The Whittle Laboratory cascade tunnel is a closed circuit, continuously running variable density facility. It is driven by a 1 MW three-stage centrifugal compressor with a pressure ratio of 2.5:1 at a mass flow rate

of 4.8 kg s^{-1} for an entry pressure of 100 kPa, and temperature of 300 K (19).

For a linear turbine cascade of around 80 cm^2 throat area the Mach number at outlet may be varied from 0.5 to 1.25 and Reynolds number is independently controllable from about 2 to 10 x 10^5 based on blade chord ($\sim$ 40 mm).

(b) Schlieren system

Both series of measurements made use of the same schlieren system with substitution of either a high-speed camera or photomultiplier detectors in the image plane.

This is a standard single pass system with two spherical mirrors of 2.4 m focal length and 0.3 m diameter. The light sources are a high pressure 100 W miniature mercury arc tube giving an effective source size of about 1 x 1 mm and a standard photographic flash gun giving an effective source size of 2 x 2 mm and a flash duration of about 1/1000s. Because of space limitations around the cascade tunnel the light beams are folded with plane mirrors both on the source and detector side. (Fig.2).

Two 'knife edges' were found effective; one was a conventional graded filter, the other was a suitably shaped opaque dot, or 'top hat' filter. The latter, essentially, produced a dark field schlieren image. This was useful in increasing signal to noise ratio in the light beam.

(c) Data acquisition

(i) Image converter camera

The very high framing rates needed to analyse motion at the trailing edges were attained by the use of an IMACON 790 image converter camera (9). Rotating mirror cameras are available which will provide framing rates up to about 10^6 pps (pictures per second) with limited portability. Their principal advantage over the image converter is their higher optical resolution, typically 20 lines per millimeter as against four or five for the image converter tube. The image converter camera, in practice, is much more convenient to use however. It may be triggered very rapidly, operates

at much lower light levels and gives a large and conveniently adjustable range of framing rates typically, from 2 x 10^5 to 10^7 pps.

3000 ASA Polaroid film was used to provide immediate assessment of the results.

The schlieren system was adjusted to give a real image of the correct size and magnification in the plane of the photosensitive surface of the image converter.

(ii) Correlator

The exit beam of the schlieren system was split to produce two image planes. In each plane a small screen was positioned. These could be moved in any direction in the image plane by means of simple lead screws rotated manually, (Fig. 3).

In the centre of each screen a 0.25 mm diameter hole fed light into a fibre optic cable. Each cable was in turn connected directly to the photosensitive surface of the photomultipliers.

Thus, the autocorrelation function of the signal from each screen could be obtained. Or the detector holes could be positioned to provide a cross correlation between two separate points in the flow field.

The photomultiplier signal after amplification and a discriminator stage,were input to the digital correlator.

The digital correlator was a Malvern type K7023. By the use of clipping techniques described in (10) the time consuming multiplications normally needed for correlation are reduced to single bit operations with a proportionate increase in speed. The resultant bandwidth is 20 MHz but, whilst clipping one of the input signals has no effect on Gaussian distributions of input pulses, the effect on other distributions is not clear except in isolated cases (10)(11).

(d) Data reduction

The treatment of correlated and autocorrelated data in general has been the object of a great deal of effort (see, for instance, (11),(12) and (13)).

Nevertheless, a few comments in the context of the present experiments are appropriate.

Correlation of optical signals using digital correlators is widely used in laser anemometry (14)(15)(10). There, as in most of the present work, this technique depends for its relative simplicity on the presence in the flow of periodic or quasi-periodic structures. Stable vortex streets in trailing edge flows are an obvious example that we discuss here.

Correlation of the schlieren image has provided two physically distinct kinds of measurement as follows:

(i) Autocorrelation

The autocorrelation function has two extremely useful properties

$$R_x(t_1,\ t_1 + z) = \lim_{n \to \infty} \frac{1}{N} \sum_{k=1}^{N} x_k(t_1)\ x_k(t_1 + z)$$

where R_x is the autocorrelation function and $x_k(t_1)$ is the light intensity at time t_1. The averaging process allows detection of any periodicity in the signal irrespective of any short term random fluctuations.

The random component of the signal, however, determines the rate of decay of the correlation. Thus, in the case of a vortex street the decay of the autocorrelation function is a measure of randomness in the vortex structure. This may be caused by emission of limited trains of vortices or reflect increasing turbulence or, similarly, a lack of spanwise coherence.

(ii) Cross-correlation

The averaging properties of the autocorrelation function extend with greater force to the cross correlation function (11). This function yields information on the presence of a signal propagating between two points, the direction of propagation and its velocity. Again, the rate of decay of the function is a measure of the randomness in the signal. By comparison with the autocorrelation-function it is possible to evaluate the change in randomness along the propagation path.

The correlator output for both types of correlation was as shown in Fig. 4 (a cross correlation). To characterise the depth of modulation a contrast function dN/N was defined. Unfortunately the background level, N, is rather arbitrary and had to be kept constant when variations of dN/N were of interest.

(e) Experimental programme

Tests were devised to evaluate these methods as far as possible in terms relevant to the probelms of turbomachinery design. The tests included

- Accurate measurement of the frequency variation of vortex shedding from turbine blades over cascade outlet Mach No. range of 0.50 to 1.24 at constant Reynolds number (7×10^5).

- Similarly, over a range of Reynolds No. of 2.8 to 9.5×10^5 at a constant outlet Mach No. of 0.91.

- Determination of the position of transition to turbulence of the boundary layer.

- General investigation of fluctuation rates and levels in the cascade.

- Trailing edge blade-to-blade cross correlation (Mach No. range 0.60 to 1.20).

- Vortex structure by traversing across the wake.

- Convection velocities in the wake

- Visualisation of the process of vortex formation in the trailing edge region over ranges of Reynolds and Mach No. as defined above.

These tests were carried out on two different experimental, highly-loaded, turbine blade profiles referred to here as RH and RJ (Fig. 5). Details of the cascades are given in Table 1.

RESULTS AND DISCUSSION

1. Image Converter Visualisation

An overall view of the cascade flow for blade RJ is shown in Fig. 6. (Blade RH is very similar to RJ and the general features of its flow pattern are little different). This was obtained with a standard spark unit at 1/3 μs.

The image converter sequence of RJ at an outlet Mach No. of 0.91 in Fig. 7 shows much more detail of the process of formation of the discrete vortices in the wakes. (All outlet Reynolds numbers are 7×10^5 based on blade chord unless otherwise specified). The frequency is immediately obtainable from the framing rate (2×10^5 pps). Direct measurement on the photograph yields a frequency of 50 kHz ± 5kHz and a velocity of 230 ms^{-1} with a similar percentage error. This error is not a fundamental limitation of the method of measurement. It is the uncertainty in the timing of the camera's pulse generator. It was not possible to carry out an accurate calibration in these experiments. But it is estimated that the error should be no more than 1 or 2% with calibration.

Several aspects of the process of vortex formation deserve notice. Firstly the well-defined discreteness of the vortices. This has often been observed before and appears to be intermittent it is certainly dependent on operating conditions and tends to degenerate into turbulence at higher Mach numbers (around 1.2). However, since the vortices would be expected to break up in the spanwise direction into smaller three dimensional structures (18), their stability in two dimensions is remarkable.

Secondly, the vortex street is strongly asymmetric as is the wake itself. (The suction surface of the blade is uppermost). However, the apparent lack of symmetry may be to some extent an artifact of the knife edge orientation, although this was placed as symmetrically as possible across the wake. It is also quite likely that each dark spot in the sequence

represents not a single vortex core but two contra rotating vortices.

The mechanism of vortex formation appears to be rather far removed from that of the conventional von Karman vortex street. It is, moreover, not clear that the fluctuations are linked to movement of the points of separation, though this cannot be excluded.

Vortex shedding is associated with strong and extremely fast density fluctuations in the recompression region of the base flow. This presumably also causes correspondingly large variations in the base pressure itself.

This visualisation method was also applied to blade RH at a Mach number of 1.0. Unlike RJ it suffers separation of the suction surface boundary layer at that outlet velocity. The effect on the trailing edge flow and vortex shedding is shown in Fig. 8.

The fluctuations in the recompression region appear to be similar to those without boundary layer separation but the process of vortex shedding is less coherent. This was confirmed by the autocorrelation measurements.

An attempt was made to observe the stability of the separation bubble associated with the shock-boundary layer interaction on the suction side of blade RJ. The shock-laminar boundary layer separation bubbles showed no observable fluctuations in the frequency range 20-80 kHz except at the turbulent re-attachment point.

2. Correlation

(a) Autocorrelation

With the probe placed approximately as shown in Fig. 9 satisfactory autocorrelations functions were obtained. Fig. 9 shows a comparison of the data at two Mach numbers for RJ and RH. This demonstrated the different wake structures of these profiles under a range of conditions very simply. Blade RJ showed generally more coherence in its vortex structure than RH. It is, however, not appropriate to speculate on the possible causes here.

Vortex shedding frequency and Mach number

The most immediately accessible data from the autocorrelation are the frequencies of vortex shedding. The variation of vortex shedding frequency for RH and RJ with outlet Mach number is shown in Fig. 10.

The shedding frequency increased with Mach number from about 30 kHz at Mach No. 0.43 to 110 kHz at 1.22. The frequencies for the two blades agreed well until just below Mach No. 1.0 when RH displayed a marked drop in frequency of 20 kHz. There also appears to be a slope discontinuity for both profiles after M = 0.95 (M = outlet Mach number).

The sudden frequency drop for RH at M = 1.0 was caused by the unusual properties of the suction surface boundary layer of RH which separated just below M = 1.0 ((1) in Fig. 10(a)) but re-attachment occurred at around M = 1.04. That this could be seen easily illustrates one of the main advantages of the present approach. The correlator samples quantitatively one or two points in the flow but the overall picture is visible and easily interpreted at all times. The low frequency shift in RH corresponds to the condition illustrated in Fig. 8.

For convenience some data on base pressures corresponding to the points in Fig. 10 (a) and (c) are presented in (b). It is unexpected that there seems to be no correlation for RH between measured base pressure and vortex shedding frequency (20).

It was expected that the violent density fluctuations observed with the image converter camera in the base flow would cause the shocks to move similarly. Very little shock movement of this kind could be seen either in the photo sequences or by autocorrelation of the shock position.

Frequency range

In view of the remarkable coherence of the vortex shedding a search was made for other possible driving frequencies in the flow field over a range from 100 Hz to several hundred kHz.

Only one other strong discrete frequency was measured. This was between 1.2 and 1.6 kHz. It was strongly dependent on Mach No. as shown in Fig. 11. It was detectable superimposed on every other feature of the flow. It is likely therefore that it is caused by periodic unsteadiness in the free shear layer at the edge of the cascade. A similar effect has been investigated by Sieverding who found a strong coupling between unsteadiness in the free shear layer and the cascade flow at a frequency of about 400 Hz (3).

Detection of laminar-turbulent transition in boundary layer

An attempt was made to locate the transition region of the suction surface boundary layer of RJ from the autocorrelation function of points at the edge of the boundary layer before and immediately after transition. The results were unfortunately inconclusive mainly because the signals were swamped by the low frequency oscillation of the free shear layer.

Wake traverse

The optical probe was traversed across the wake of RH 5 trailing edge thicknesses downstream of the trailing edge. The traverse path was from pressure to suction side. Fig. 12 shows the variation of dN/N across the wake in agreement with similar results by Lawaczeck et al (17).

(b) Cross Correlation

Velocity in the wake

The optical probes were placed a known distance apart in the wake and the cross correlation function was obtained. First the probes sampled the wake at the same point in their respective image planes. One probe was kept stationary while the other was then moved downstream in steps of 0.5 mm. As expected the delay in the peak of the correlation depended on probe separation. This is shown in Fig. 13 (a) and (b). Delay is plotted against probe separation in (c). The calculated mean velocity (blade RH) at M = 0.91 was found to be 225 ms^{-1} . The velocity could also

be obtained directly from an image converter sequence. The result was $210 \pm 20\ ms^{-1}$. As expected, it was found that the correlation contrast (dN/N) decreased with increasing probe separation. dN/N dropped from 0.5 for autocorrelation to 0.14 for a 2 mm separation between sampling points. It was also possible to detect the decrease in wake velocity over 2 mm from the curvature of the line in (c).

Blade-to-Blade correlation

If the high level of coherence of the trailing edge vortices is maintained by some other oscillation in the cascade it is informative to cross correlate different blade trailing edge flows. This was done for blade RH by positioning the optical probes in corresponding spots in two adjacent trailing edge flows, that is, just downstream of the recompression region.

The Mach number was varied between 0.5 and 1.15 at a constant Reynolds number of 7×10^5 and the cross correlation functions were obtained. Fig. 14 (a) and (b) indicate the variation in observed delay at the peak of the correlation as a function of Mach number. The delay was reduced from 135 μs at M = 0.98 to 68 μs at M = 1.20. This general trend is to be expected. The exact mechanism for the propagation of the information from one trailing edge to the other is not clear. Fig. 14 (c) provides some help. Although the autocorrelations at subsonic Mach numbers are strong the trailing edge to trailing edge cross correlations are weak until choking occurs. It seems likely that formation of the passage shock is connected with the sudden steep increase in cross correlation. When the cross correlation direction was reversed, so that it would have detected 'information' moving upstream, no correlation was observed. The rapid decrease in correlation beyond M = 1.0 is probably caused by the increasing level of turbulence. These measurements rule out any simple mechanism like acoustic resonance as the cause of the coherence of the vortex streets. An estimate of the time taken by a pulse to travel from one trailing edge

to the other only agrees with the data in order of magnitude no close agreement is obtainable for any reasonably simple propagation path.

CONCLUSIONS

Some significant aspects of transonic cascade flow require fast response instrumentation for their investigation and measurement. Effective bandwidths of up to 1 MHz are convenient for the study of fluctuation and vortex shedding in trailing edge flows at transonic Mach numbers.

The two methods discussed in this study both meet these requirements. Very high speed photography simply exploits the intuitively accessible schlieren visualisation. It has shown even with the limitations of a brief series of tests that there may be such large unsteady effects in the trailing edge region that no model based entirely on analysis of a steady flow will be adequate to evaluate trailing edge loss.

The method of correlation of points in the schlieren image was extremely convenient for the measurement of periodic components in the flow. In addition it ruled out immediately any over simplified acoustic resonance models to explain the high coherence of the trailing edge vortex streets. It should perhaps be underlined that these measurements made use of the extremely high sensitivity of the photon correlation method. It does not rule out the use of other, more conventional correlators.

It became clear that problems of interpretation of the correlations arise when the exact statistical properties of the input signal are required, as they would be in an investigation of turbulence.

ACKNOWLEDGMENTS

J-J Camus thanks Rolls-Royce Limited for their interest and support of the cascade facility.

P.J. Bryanston-Cross thanks the Central Electricity Generating Board for their support and Dr. P.H. Richards for useful discussions.

We also thank Dr. D.S. Whitehead and Professor J.E. Ffowcs Williams for their comments.

REFERENCES

1. K. Finke
"Stobschwingungen in schallnahen Strömungen"
V.D.I. Forschungsheft 580, 1977, pp 3-39

2. W.M. Jungowski
"Some Self-induced Supersonic Flow Oscillations"
Progress in Aerospace Sciences, Vol. 18, pp 151-175.

3. C.H. Sieverding
"Unsteady Flow Measurements in Straight Cascades"
Measuring Techniques in Transonic and Supersonic Cascades and Turbomachines
eds. A. Bölcs and T. Fransson
Juris-Verlag, Zürich, 1977

4. G. Comte-Bellot
"Hot Wire and Hot Film Anemometers"
in Measurements of Unsteady Fluid Dynamic Phenomena
B.E. Richards ed., McGraw-Hill, 1977.

5. M.L.G. Oldfield, R. Kiock, A.T. Holmes, C.G. Graham
"Boundary layer studies on Highly-Loaded Cascades using Heated Thin Films and a Traversing Probe"
Journal of Engineering for Power, Trans. ASME, Vol. 103, Jan. 1981, pp 237-246.

6. H.-J Heinemann and K.A. Bütefisch
"Determination of the Vortex Shedding Frequency of Cascades with Different Trailing Edge Thicknesses".
AGARD CP-277 (1978)
Proc. Agard FDP Conference, Ottawa, Canada, Sept. 1977.

7. O. Lawaczeck and H.-J Heinemann
"von Karman Vortex Streets in the Wakes of Subsonic and Transonic Cascades"
AGARD-PEP Meeting, Unsteady Phenomena in Turbomachinery
AGARD CP-177, 1975.

8. C.G. Graham and F. Kost,
"Shock-Boundary Layer Interaction on High Turning Transonic Turbine Cascades".
ASME Paper No. 79-GT-37, 1979.

9. IMACON manufacturer reference . John Hadland P.T.J., Bovingdon, Essex, U.K.

10. E.R. Pike
"Photon Correlation Velocimetry"
in Photon Correlation, Spectroscopy and Velocimetry
H.Z. Cummins and E.R. Pike eds.
Plenum Press, N.Y., 1977.

11. J.S. Bendat and A.G. Piersol
"Random Data: Analysis and Measurement Procedures"
Wiley-Interscience, New York, 1971.

12. A. Papoulis
"Probability, Random Variables and Stochastic Processes"
McGraw-Hill Inc., 1965.

13. D.E. Newland
"An Introduction to Random Vibrations and Spectral Analysis"
Longman, London, 1975.

14. C.J. Oliver
"Correlation Techniques"
in "Photon Correlation and Light Beating Spectroscopy"
H.Z. Cummins and E.R. Pike eds.,
Plenum Press, N.Y., 1974.

15. A.E. Smart
"Data Retrieval in Laser Anemometry by Digital Correlation"
Third Int. Workshop on Laser Velocimetry, Purdue Un. Lafayette,
Indiana, 11-13 July, 1978.

16. O. Lawaczeck, K.A. Bütefisch and H.-J Heinemann
"Vortex Streets in the Wakes of subsonic and transonic turbine cascades"
Revue Française de Mécanique suppl to proceedings of IUTAM
Symp. on Aeroelasticity in Turbomachines, ENSTA, Paris, 1976.

17. N.A. Cumpsty and D.S. Whitehead
"The Excitation of Acoustic Resonances by Vortex Shedding"
J. Sound and Vibration, 18 (3), 353-369, 1971

18. J.P. Gostelow and P.J. Watson
"A closed Circuit Variable Density Air Supply for Turbomachinery Research"
ASME Paper No. 76-GT-62, 1976

19. J.F. Nash, V.G. Quincey and J. Callinan
"Experiments on Two-Dimensional Base Flow at Subsonic and Transonic Speeds"
NPL Aero Rept. 1070, ARC 25070, FM 3356, National Physical Laboratory,
Jan. 1963.

TABLE 1

CASCADES AND TEST CONDITIONS

	RH	RJ
Blade chord (mm)	41.7	41.7
s/c	0.834	0.834
d/c	0.04	0.04
Aspect ratio	2.44	2.44
Inlet angle	59.1	59.1
Outlet angle	70.8	71.4
No. of Blades	6	6
Inlet Stagnation Pressure	50-150 kPa	
Inlet stag. Temp. (K)	300	
Inlet turbulence	0.5 - 1.0 (% r.m.s.)	
Outlet Mach No.	0.5 - 1.25	
Outlet Reynolds No. based on true chord	7×10^5	

s = pitch

c = true chord

d = trailing edge thickness

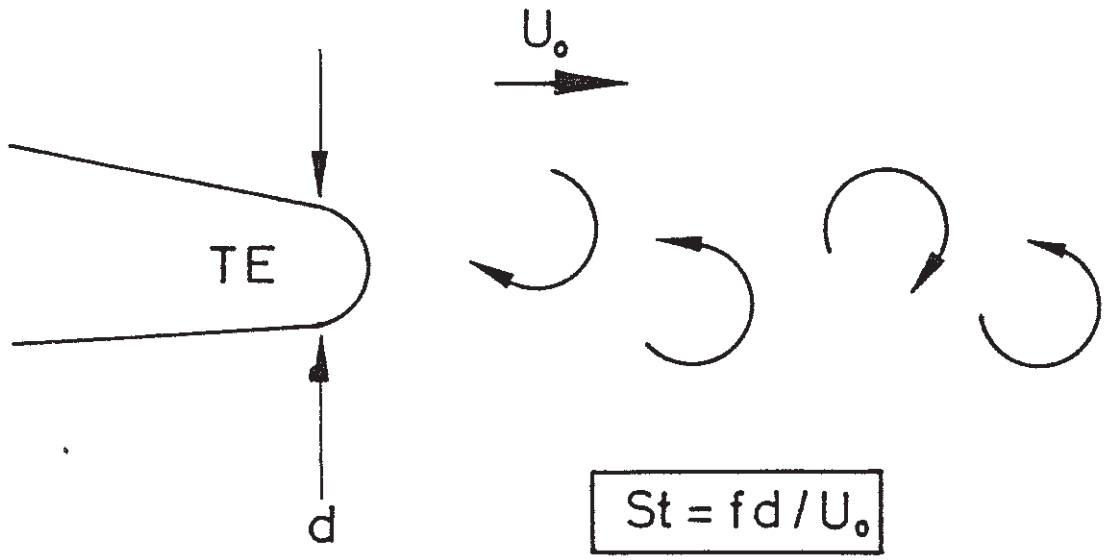

Stable Vortex Street: St = 0.2

if U_o = 340 m/s & d = 1 mm frequency = 68 kHz

Fig 1

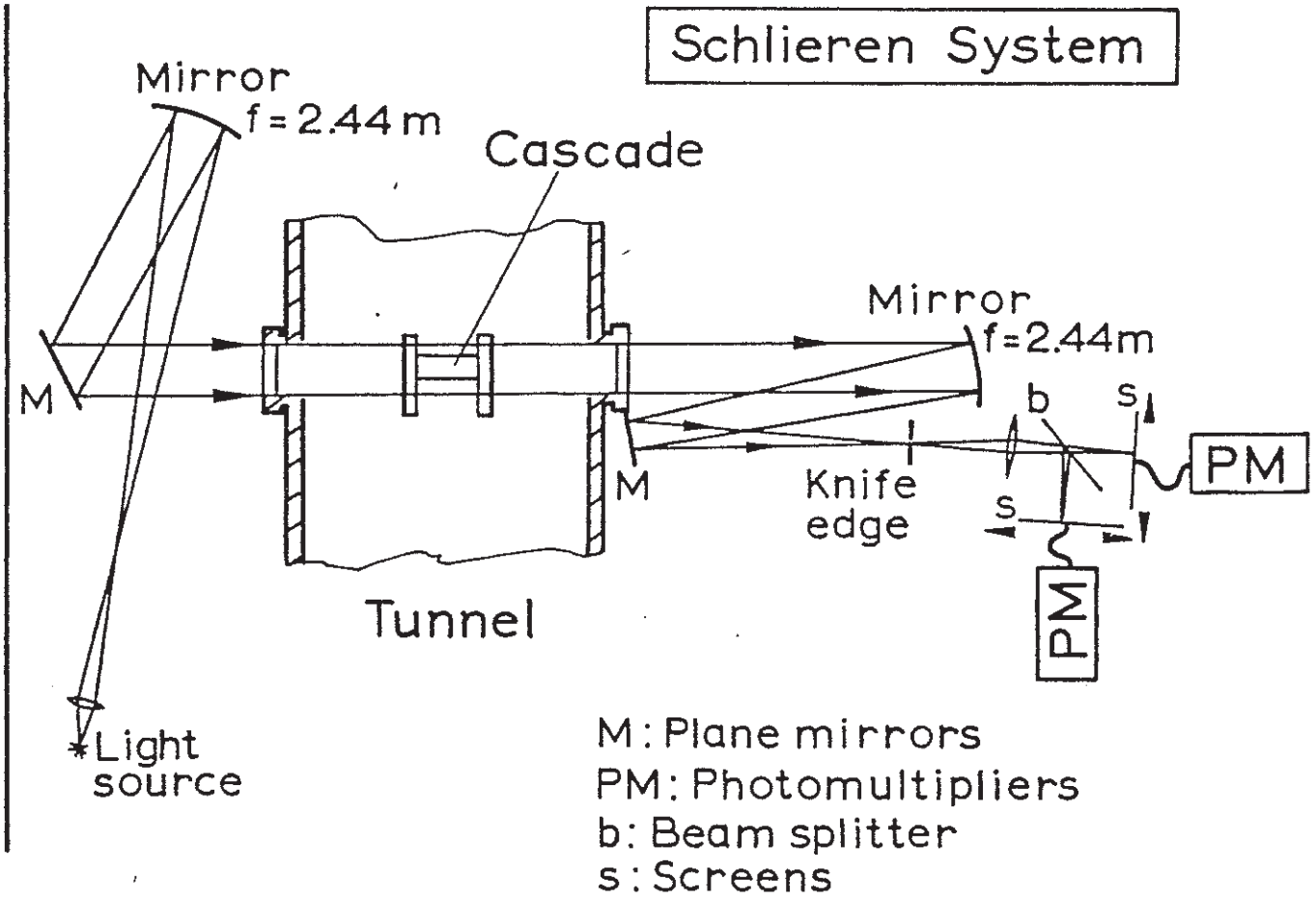

Fig 2

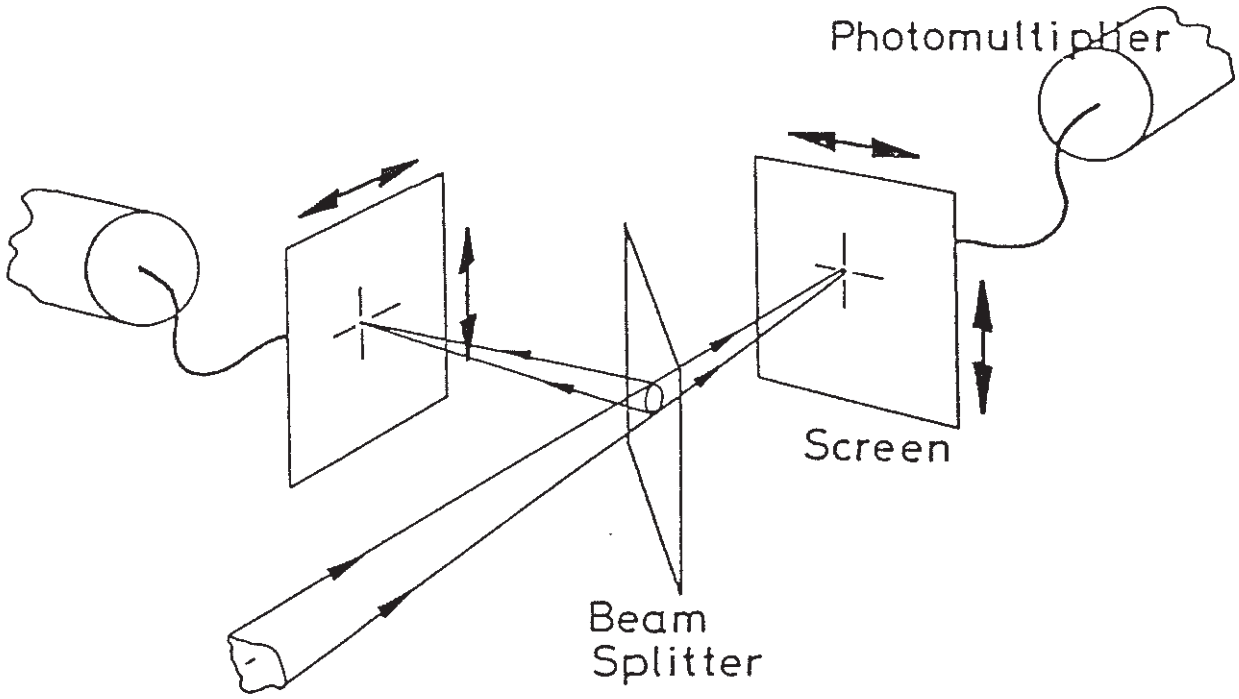

Fig 3 Beam Splitter / Screens

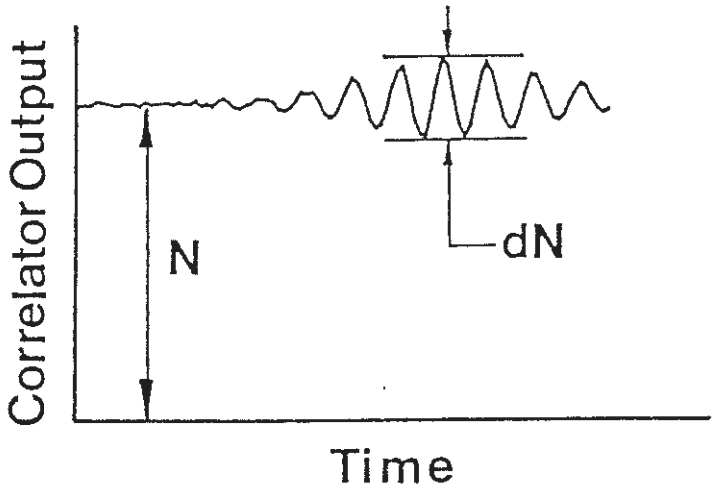

Fig 4 Definition of Correlation Contrast

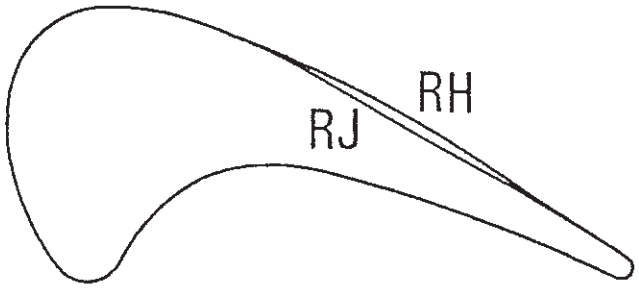

Fig 5 Blade Profiles

FIG. 6 VORTEX STREETS IN RJ PROFILE WAKES
MA2 = 0.90 Re = 7 x 10^5

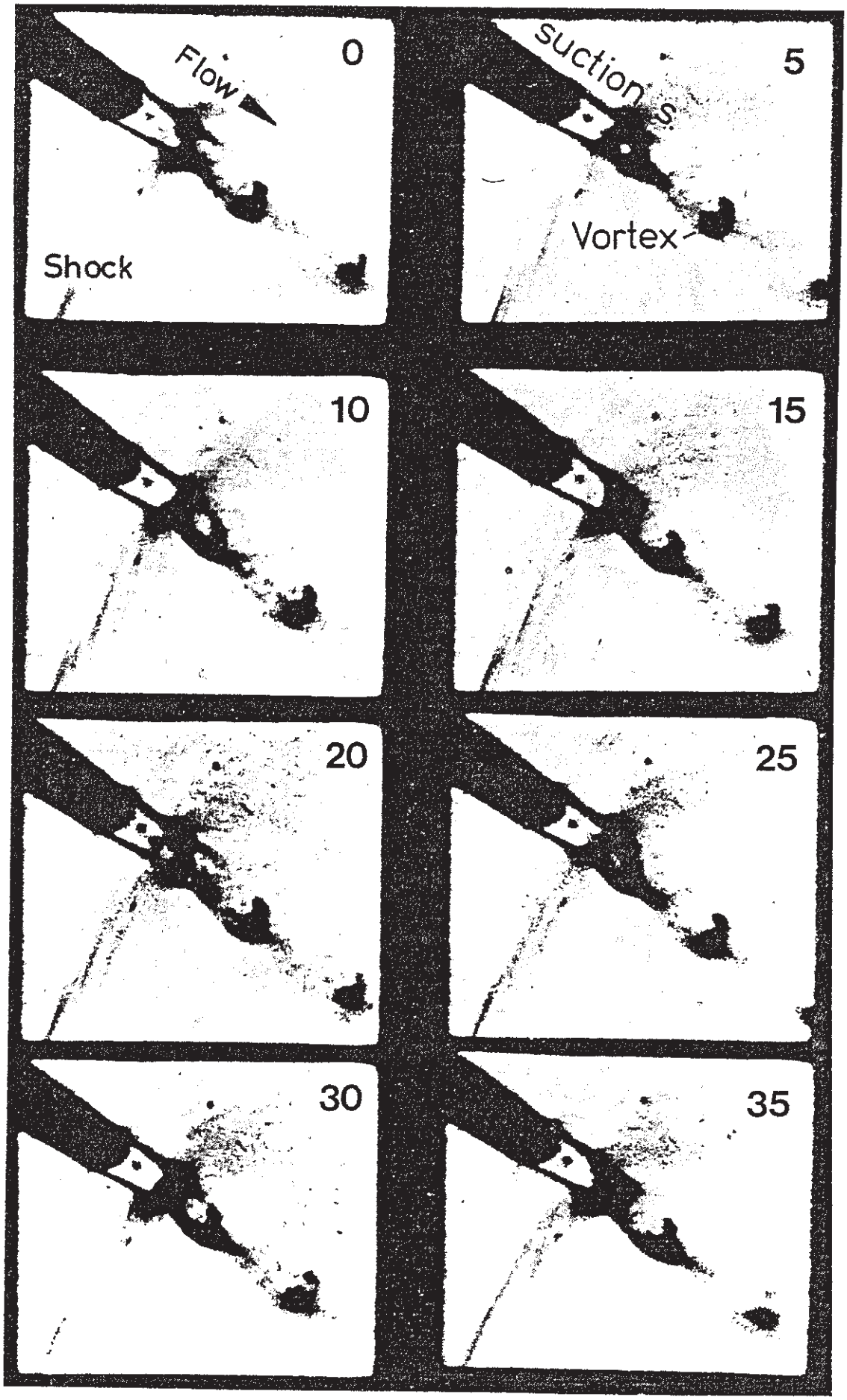

FIG. 7 VORTEX SHEDDING FROM TRAILING EDGE OF PROFILE RJ. FRAMES MARKED IN μ SECS. M = 0.91, Re2 = 7 x 10^5

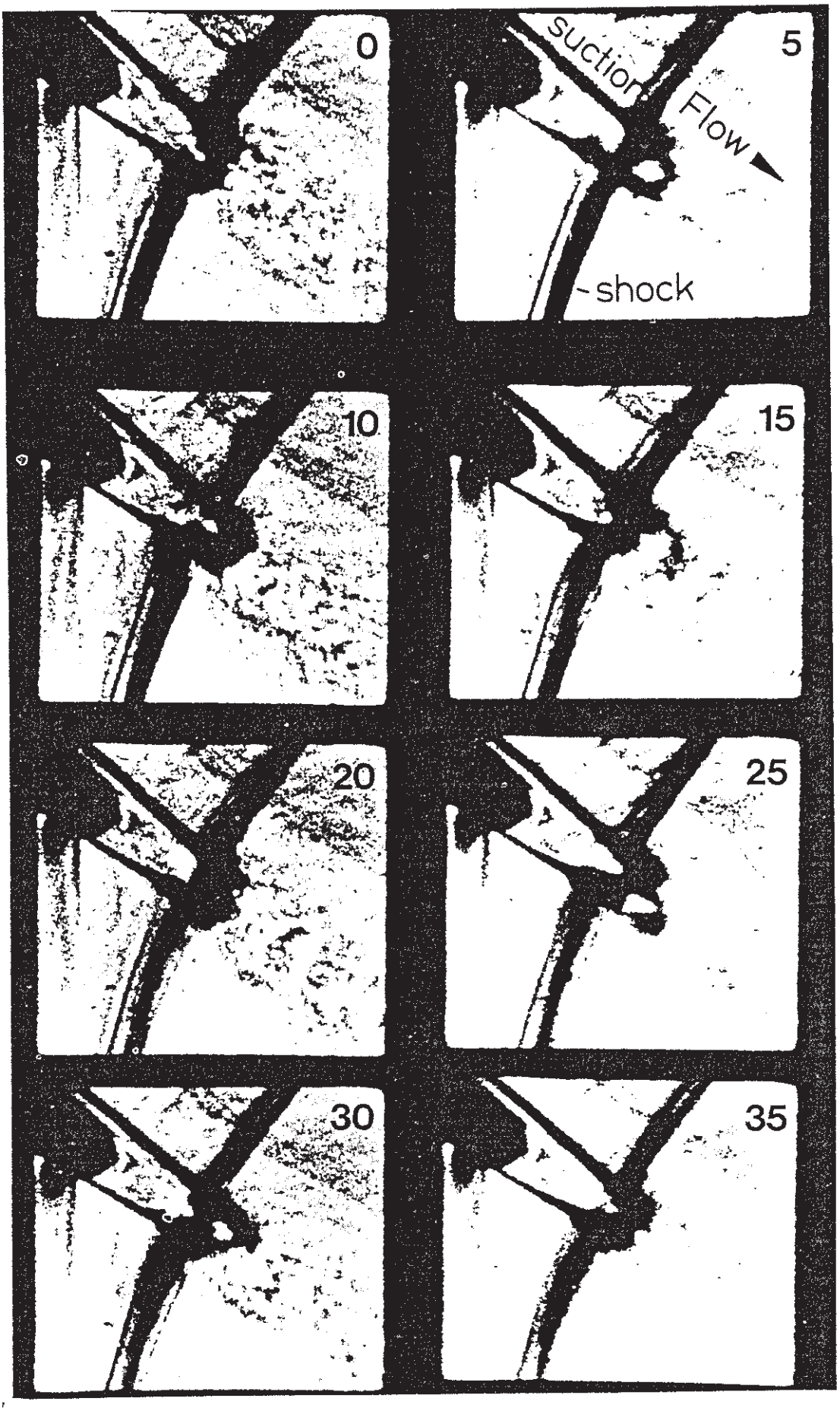

FIG. 8 VORTEX SHEDDING FROM TRAILING EDGE OF PROFILE RH
FRAMES MARKED IN μ SECS. M = 0.91, Re 2 = 7 x 10^5

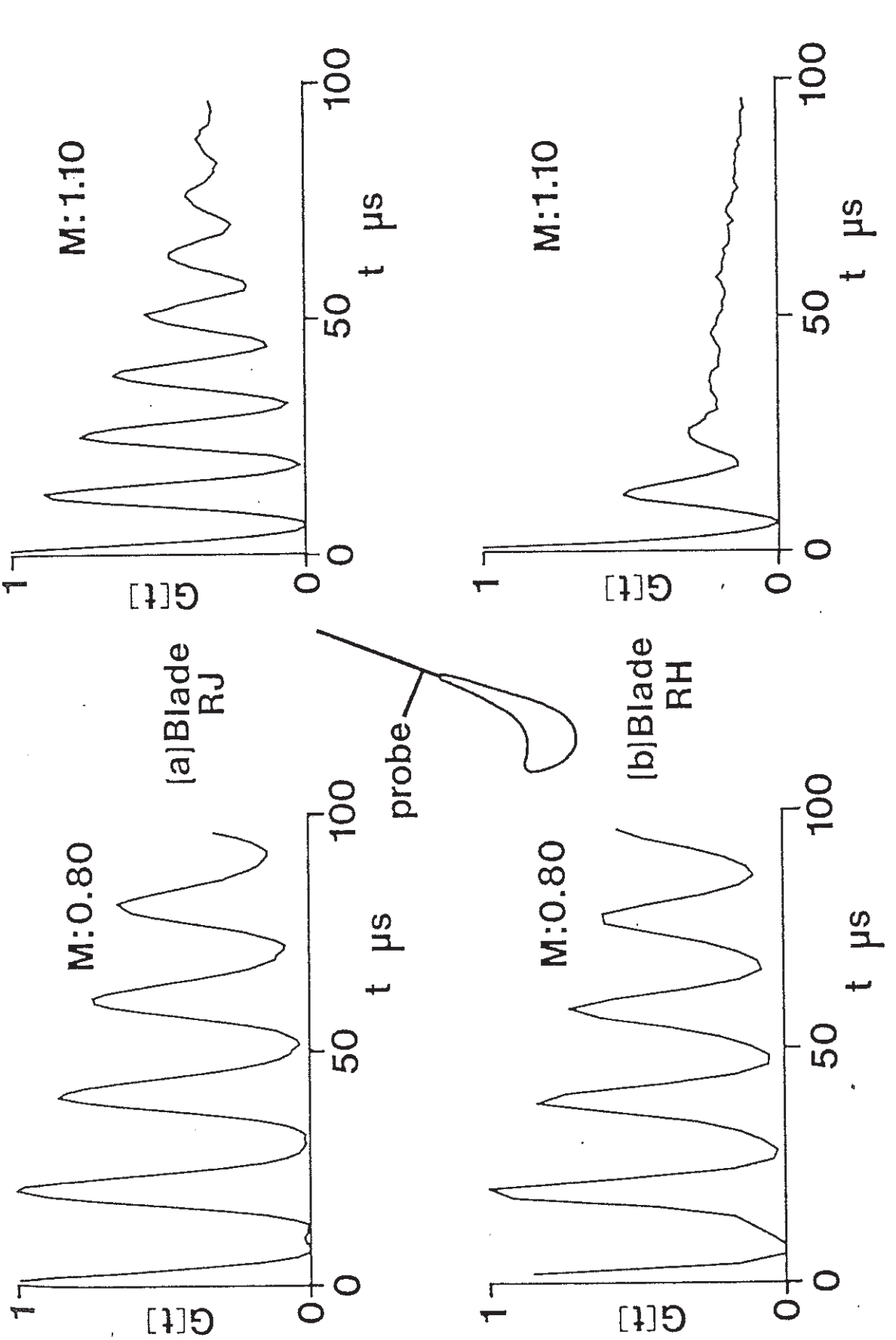

FIG. 9 AUTOCORRELATIONS IN THE WAKES OF PROFILES RJ AND RH. THE DIFFERENT DECAY RATES ARE A FUNCTION OF DIFFERENCES IN THE BOUNDARY LAYERS OF RH AND RJ.

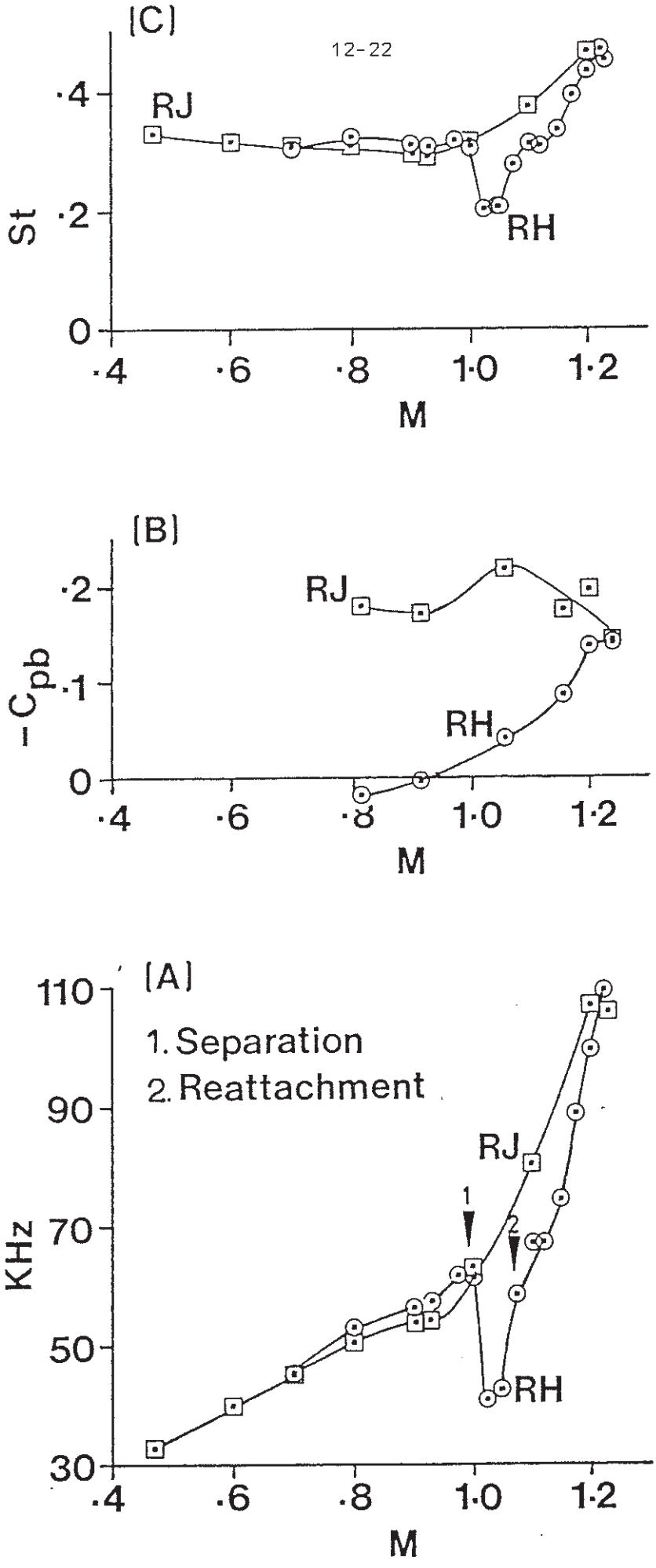

FIG. 10 VARIATION OF VORTEX SHEDDING FREQUENCY (A), BASE PRESSURE COEFFICIENT (B), STROUHAL NO. (C) WITH MACH NO. PROFILE RH

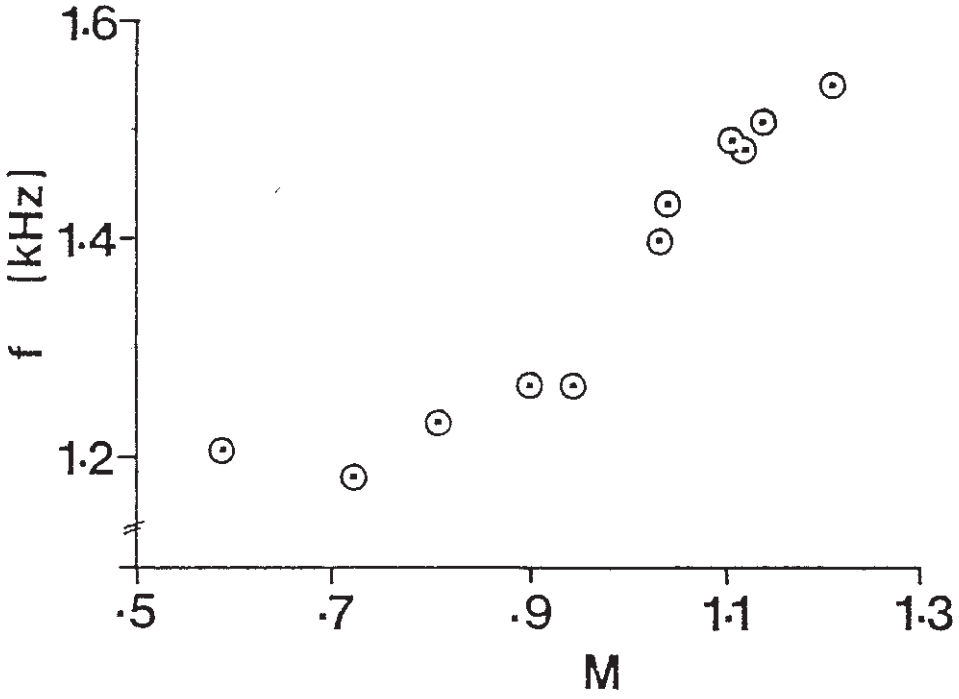

FIG. 11 VARIATION WITH MACH NO. OF LOW FREQUENCY COMPONENT OF CASCADE FLUCTUATIONS.

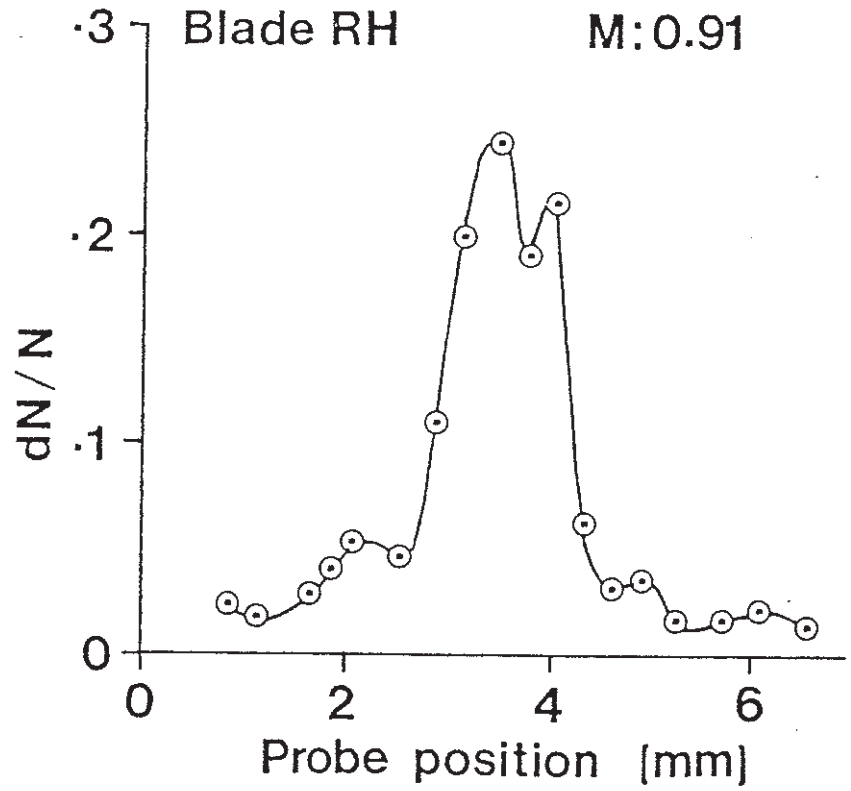

FIG. 12 VARIATION IN AUTO CORRELATION LEVEL ACROSS WAKE 5 TRAILING EDGE THICKNESSES DOWNSTREAM.

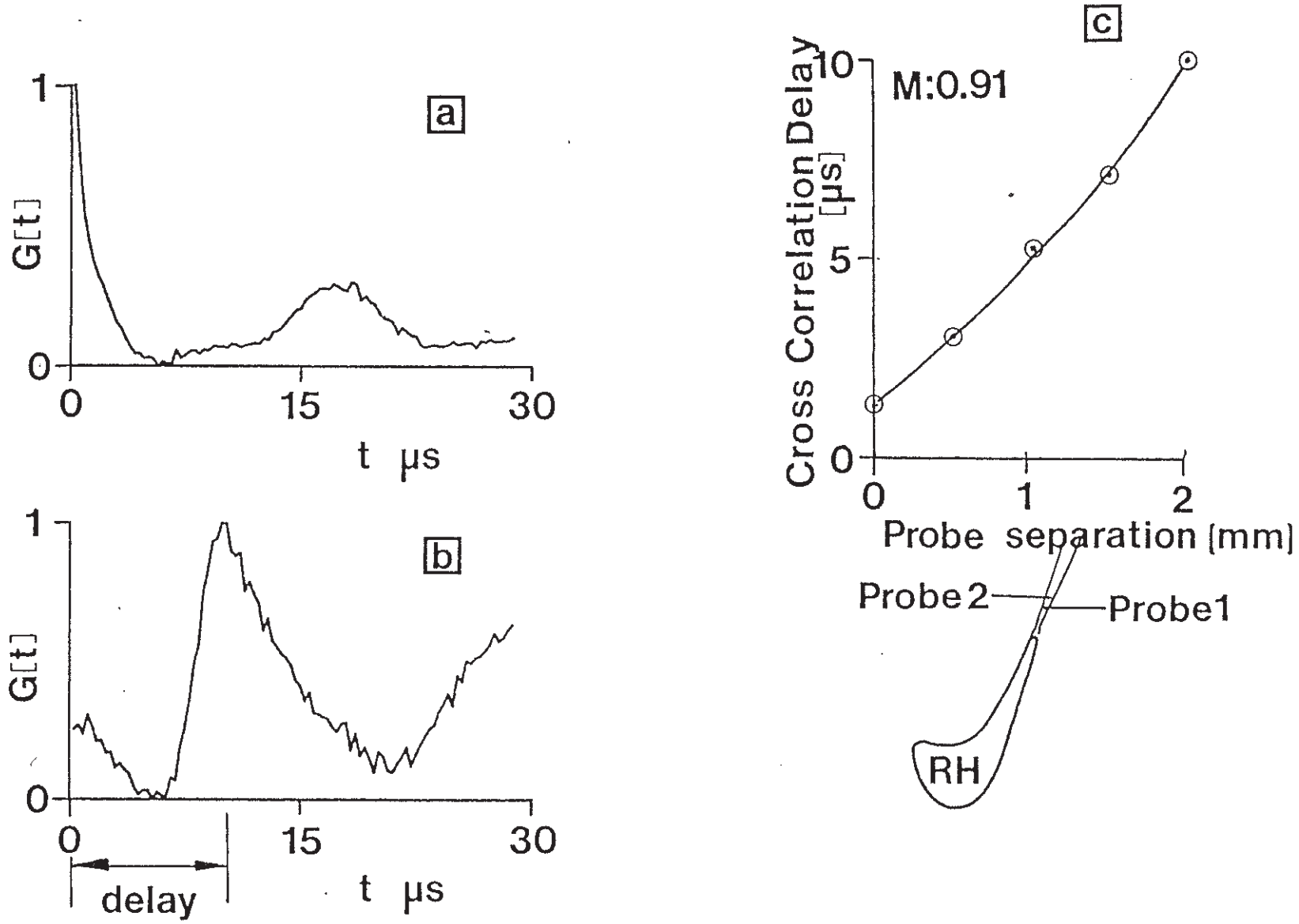

FIG. 13 VELOCITY IN THE WAKE BY CORRELATION: (A) AUTO-CORRELATION OF PROBE 1. (B) CROSS CORRELATION BETWEEN PROBES 1 & 2. (C) DELAY TIME AS A FUNCTION OF PROBE SEPARATION.

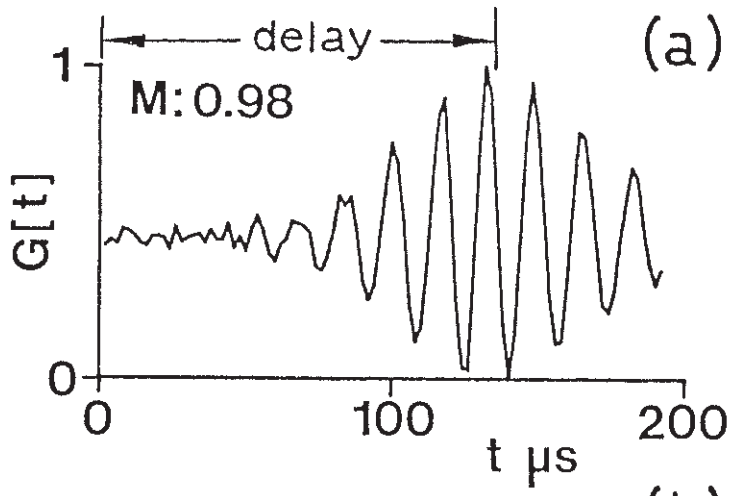

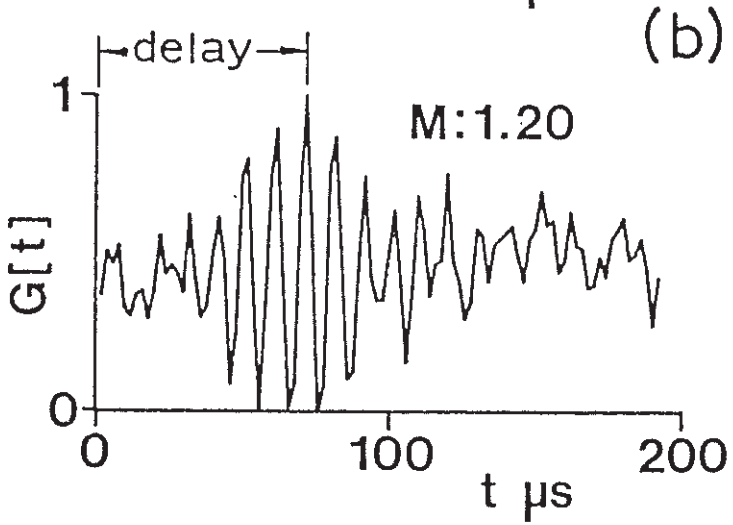

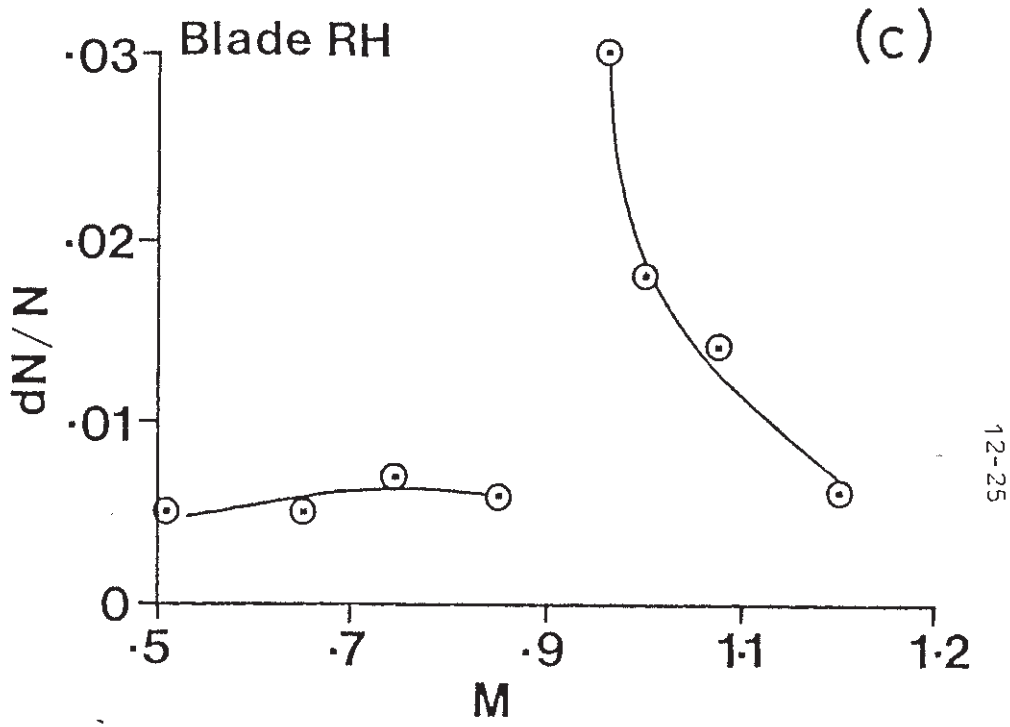

12-25

FIG. 14 WAKE-TO-WAKE CROSS CORRELATION SHOWING DEPENDENCE OF DELAY ON MACH NO. (c) SHOWS STRENGTH OF CORRELATION AS A FUNCTION OF MACH NO.